doi:10.1093/brain/awr338 Brain 2012: 135; 506–520 | 506

BRAIN
A JOURNAL OF NEUROLOGY

Connexin43 mimetic peptide reduces vascular leak and retinal ganglion cell death following retinal ischaemia

Helen V. Danesh-Meyer,[1] Nathan M. Kerr,[1] Jie Zhang,[1] Elizabeth K. Eady,[1] Simon J. O'Carroll,[2,3] Louise F.B. Nicholson,[2,3] Cameron S. Johnson[1] and Colin R. Green[1]

1 Department of Ophthalmology, Faculty of Medical and Health Sciences, University of Auckland, Auckland 1142, New Zealand
2 Department of Anatomy with Radiology, Faculty of Medical and Health Sciences, University of Auckland, Auckland 1142, New Zealand
3 The Centre for Brain Research, Faculty of Medical and Health Sciences, University of Auckland, Auckland 1142, New Zealand

Correspondence to: Professor Helen V. Danesh-Meyer,
MBChB, MD, FRANZCO,
Department of Ophthalmology, University of Auckland,
Private Bag 92019, Auckland Mail Centre,
Auckland 1142, New Zealand,
E-mail: h.daneshmeyer@auckland.ac.nz

Connexin43 gap junction protein is expressed in astrocytes and the vascular endothelium in the central nervous system. It is upregulated following central nervous system injury and is recognized as playing an important role in modulating the extent of damage. Studies that have transiently blocked connexin43 in spinal cord injury and central nervous system epileptic models have reported neuronal rescue. The purpose of this study was to investigate neuronal rescue following retinal ischaemia-reperfusion by transiently blocking connexin43 activity using a connexin43 mimetic peptide. A further aim was to evaluate the effect of transiently blocking connexin43 on vascular permeability as this is known to increase following central nervous system ischaemia. Adult male Wistar rats were exposed to 60 min of retinal ischaemia. Treatment groups consisted of no treatment, connexin43 mimetic peptide and scrambled peptide. Retinas were then evaluated at 1–2, 4, 8 and 24 h, and 7 and 21 days post-ischaemia. Evans blue dye leak from retinal blood vessels was used to assess vascular leakage. Blood vessel integrity was examined using isolectin-B4 labelling. Connexin43 levels and astrocyte activation (glial fibrillary acidic protein) were assessed using immunohistochemistry and western blot analysis. Retinal whole mounts and retinal ganglion cell counts were used to quantify neurodegeneration. An *in vitro* cell culture model of endothelial cell ischaemia was used to assess the effect of connexin43 mimetic peptide on endothelial cell survival and connexin43 hemichannel opening using propidium iodide dye uptake. We found that retinal ischaemia-reperfusion induced significant vascular leakage and disruption at 1–2, 4 and 24 h following injury with a peak at 4 h. Connexin43 immunoreactivity was significantly increased at 1–2, 4, 8 and 24 h post ischaemia-reperfusion injury co-localizing with activated astrocytes, Muller cells and vascular endothelial cells. Connexin43 mimetic peptide significantly reduced dye leak at 4 and 24 h. *In vitro* studies on endothelial cells demonstrate that endothelial cell death following hypoxia can be mediated directly by opening of connexin43 hemichannels in endothelial cells. Blocking connexin43 mediated vascular leakage using a connexin43 mimetic peptide led to increased retinal ganglion cell survival at 7 and 21 days to levels of uninjured retinas. Treatment with scrambled peptide did not result in retinal ganglion cell rescue. Pharmacological targeting of connexin43 gap junction protein by transiently blocking gap junction hemichannels following injury provides new opportunities for treatment of central nervous system ischaemia.

Received June 28, 2011. Revised October 14, 2011. Accepted November 1, 2011

Keywords: connexin43; central nervous system ischaemia; retinal ischaemia; retinal ganglion cells; neuroprotection
Abbreviations: GFAP = glial fibrillary acidic protein

Introduction

Connexin43, a ubiquitous CNS gap junction protein expressed in astrocytes and the vascular endothelium, is recognized as playing an important role in modulating the response to CNS injury. Six connexin units form a connexon, or hemichannel, that binds to an analogous structure on a neighbouring cell to form a gap junction. Gap junctions couple astrocytes to form a glial syncytium (Naus *et al.*, 1991; Rouach *et al.*, 2002). Connexin43 gap junctions also contribute to the coupling and coordinated response produced by the endothelial cell network (DePaola *et al.*, 1999; Yeh *et al.*, 2000). Under normal physiological conditions, the glial network is said to be responsible for the spatial buffering of ions and signalling molecules to maintain homeostasis (Nagy and Rash, 2000; Zahs *et al.*, 2003).

Investigations have demonstrated that connexin43 gap junctions are involved in the earliest cellular responses to injury, although the precise role remains controversial. Some studies have reported that connexin43 gap junctional communication is associated with the spread of cell death signals (Garcia-Dorado *et al.*, 1997; Lin *et al.*, 1998; Frantseva *et al.*, 2002*b*; Cronin *et al.*, 2008; Rawanduzy *et al.*, 2009), while others have demonstrated neuroprotective effects (Naus *et al.*, 2001; Nakase *et al.*, 2004). Following CNS injury, there is a well defined astrocytic response consisting of rapid proliferation, hypertrophy and changes in the expression of glial fibrillary acidic protein (GFAP), along with upregulation of connexin43 expression (Rouach *et al.*, 2002; Lee *et al.*, 2005). This upregulation of connexin43 expression following CNS ischaemia may amplify the initial damage through spreading of deleterious material from dead or dying cells to healthy neighbours (Frantseva *et al.*, 2002*a*, *b*). Activation of astrocytes subsequent to CNS injury may induce degeneration of neurons and compromise the structure of blood vessels (Shen *et al.*, 2010). Under ischaemic conditions, unopposed hemichannels can also open and form a direct link between the intracellular and extracellular milieu (Rouach *et al.*, 2002; Goodenough and Paul, 2003). An increase in connexin43 immunoreactivity levels has been described following stroke (Nakase *et al.*, 2006), brain ischaemia (Hossain *et al.*, 1994; Haupt *et al.*, 2007), traumatic brain injury (Ohsumi *et al.*, 2006) and spinal cord injury (Lee *et al.*, 2005).

Recently, gap junction modulation has been identified as a potential neuroprotective target (Frantseva *et al.*, 2002*a*, *b*; Cronin *et al.*, 2008; Danesh-Meyer *et al.*, 2008; O'Carroll *et al.*, 2008; De Bock *et al.*, 2011) with gap junction inhibitors protecting retinal neurosensory cells from ischaemia in a cell culture model (Das *et al.*, 2008). More specific blockers of connexin43 have also been investigated. Transient blocking of connexin43 following injury has been demonstrated to show some neuroprotective effects. In an *in vitro* interphase organotypic culture model of optic nerve ischaemia, application of connexin43 antisense oligodeoxynucleotide treatment downregulated neuroinflammation (Danesh-Meyer *et al.*, 2008). Application of the connexin43 antisense oligodeoxynucleotide has also been shown to reduce spinal cord swelling and disruption with better behavioural scores in two models of spinal cord injury (Cronin *et al.*, 2008). A different approach has been to use mimetic peptides, small amino acid sequences designed to bind to extracellular regions of the connexin43 protein thereby inhibiting hemichannel opening and gap junction communication. Connexin43 mimetic peptides have proven successful in preventing hemichannel opening-dependent dye uptake and reducing the spread of damage following CNS injury (O'Carroll *et al.*, 2008) and cardiac ischaemia (Hawat *et al.*, 2010), and in preventing vascular leak both *in vitro* and *in vivo* after application of the inflammatory peptide bradykinin (De Bock *et al.*, 2011). In an *ex vivo* model of hippocampal slice cultures induced to demonstrate epileptiform activity, connexin43 mimetic peptide resulted in decreased epileptiform activity (Yoon *et al.*, 2010).

The current investigation set out to assess whether blocking connexin43 channels with a systemically delivered connexin43 mimetic peptide produces neuroprotective effects for retinal ganglion cells in a model of retinal ischaemia-reperfusion. Similar to the brain and spinal cord, connexin43 is expressed on astrocytes in the retinal ganglion cell layer and optic nerve, Muller cells, and endothelial cells in the retinal and choroidal vasculature (Kerr *et al.*, 2010). The retinal ganglion cell death that occurs with retinal ischaemia is implicated in the pathology of conditions such as central retinal artery/vein occlusion, diabetic retinopathy and glaucoma. Retinal ischaemia-reperfusion has been shown to produce an increased vascular permeability of the endothelial cell network at the blood–retinal barrier evident from 4 h (Wilson *et al.*, 1995; Zheng *et al.*, 2007; Abcouwer *et al.*, 2010), with subsequent retinal ganglion cell degeneration (Osborne *et al.*, 2004; Zheng *et al.*, 2007).

We hypothesized that the upregulation of connexin43 that occurs following retinal ischaemia-reperfusion in retinal astrocytes, Muller cells and the vascular endothelium is involved in the induction of neuronal cell death and that application of a connexin43 mimetic peptide blocker would lead to neuronal rescue. Following retinal ischaemia-reperfusion animals were randomized into three groups: no treatment, connexin43 mimetic peptide or scrambled peptide. In addition, *in vitro* assays were performed on primary rat brain microvascular endothelial cells and human dermal microvascular endothelial cells (HMEC-1) to investigate the effect of connexin43 mimetic peptide on endothelial cell survival after ischaemia. We discovered that retinal ischaemia causes connexin43 mediated vascular leakage that leads to the loss of retinal ganglion cells by Day 21. Blocking connexin43 hemichannels using a connexin43 mimetic peptide rescued retinal ganglion cells with no significant difference to uninjured retinas.

Materials and methods

Animal model

All procedures were conducted in compliance with the ARVO Statement of Use of Animals in Ophthalmic and Vision Research and were approved by the Animal Ethics Committee of the University of Auckland. One hundred and fifty adult male Wistar rats weighing 250–300 g were obtained from the Vernon Janson Unit of the University of Auckland and housed with a 12-h light/dark cycle and received food and water *ad libitum*. Table 1 shows the number of animals used in each experiment.

Connexin43 mimetic peptide design

The rat connexin43 mimetic peptide design was derived from previous studies (O'Carroll *et al.*, 2008). Connexin43 mimetic peptide (sequence VDCFLSRPTEKT) has been shown to block connexin43 gap junction channels following CNS injury (O'Carroll *et al.*, 2008). A scrambled sequence of connexin43 mimetic peptide (sequence RFKPSLCTTDEV) was used as a scrambled peptide control. Peptides were custom manufactured by Auspep, Australia. Peptides were synthesized by solid phase using Fmoc chemistries on a Protein Technologies, Symphony® instrument. Peptides were purified by high performance liquid chromatography and the structures confirmed by analytical high performance liquid chromatography and mass spectral analysis.

Table 1 Number of eyes analysed in each experimental group

Number of retinas analysed (one retina per animal)			
	No treatment	Connexin43 mimetic peptide	Scrambled peptide
Evans blue dye leak			
Controls	6 uninjured + 2 no dye		
1–2 h	4		
4 h	7	7	
24 h	5	7	
Connexin43/GFAP immunohistochemistry			
Controls	4 uninjured		
1–2 h	4		
4 h	3		
8 h	4		
24 h	4		
Retinal ganglion cell whole mounts			
Controls	5 uninjured		
7 days	12	15	12
21 days	14	12	11
GFAP western blot			
Controls	2 uninjured		
8 h	2	2	2
Vascular integrity isolectin-B4 analysis			
Controls	2 uninjured		
4 h	2		

Total $n = 150$.

Retinal ischaemia-reperfusion model and treatment

Animals were anaesthetized with an intraperitoneal injection of ketamine (60 mg/kg) and medetomidine hydrochloride (0.4 mg/kg) and the cornea anaesthetized with oxybuprocaine hydrochloride (0.4%). The technique of retinal ischaemia-reperfusion has previously been described (Sun *et al.*, 2007). Briefly, the left anterior chamber was cannulated with a 30-gauge infusion needle connected by silicone tubing to a reservoir of sterile 0.9% saline. Cannulation was performed using a stereotaxic manipulator arm to avoid injury to the corneal endothelium, iris or lens. The intraocular pressure of the cannulated eye was raised to 120 mmHg for 60 min by elevating the saline reservoir. Retinal ischaemia-reperfusion was confirmed by pallor of the posterior segment. After 60 min, the cannula was removed and reperfusion of the retinal vessels was confirmed by ophthalmoscopy. Three experimental groups were applied at the end of 60 min of ischaemia. These included no treatment, connexin43 mimetic peptide, or scrambled peptide. Systemic delivery of 1 ml of a 2-mM connexin43 mimetic peptide or scrambled peptide solution diluted in 0.9% saline was achieved through intraperitoneal delivery at the start of reperfusion. A final blood peptide concentration of 100 μM was intended, assuming a blood volume of 20 ml and total systemic uptake of peptide. At various times after reperfusion (1–2, 4, 8 and 24 h, and 7 and 21 days), animals were euthanized with CO_2.

Evans blue dye leak

Vascular leak following retinal ischaemia-reperfusion was assessed using Evans blue dye (E2129, Sigma Aldrich), an azo dye that binds to serum albumin and is used to quantify vascular endothelium permeability. It was prepared in 0.9% saline at a concentration of 100 mg/ml and filtered through a 0.22-μm filter prior to administration. The dye solution was injected intraperitoneally at 1 ml/100 g of animal body weight, 10 min before the animal was due to be culled in order to allow absorption of the dye and circulation throughout the body. The dye concentration, volume injected and latent period were based on results from preliminary investigations. Animals were assessed in the control uninjured group, and 4 and 24 h following reperfusion in both treatment groups (connexin43 mimetic peptide and no treatment). Animals were culled and eyes enucleated at the respective times. The cornea, lens and vitreous humour were removed, and the remaining retina and sclera fixed in 4% paraformaldehyde in phosphate-buffered saline (BR0014G, Oxoid) for 30 min at room temperature. The fixed retina was carefully removed from the sclera and mounted onto a SuperFrost® Plus slide (Menzel-Glaser) using Citifluor™ mounting medium, before imaging.

In vitro assays

In order to establish the mechanism by which vascular leak was occurring and the link with connexin43 expression, an *in vitro* endothelial cell assay was used with a modified protocol from Zhou *et al.* (2010). Rat brain microvascular endothelial cells (R840K-05a, Cell Applications) were plated into 24-well plates (1×10^5 cells/well) in rat brain microvascular endothelial cell growth media (R819K-500, Cell Applications) and allowed to settle for 16 h. Medium was then removed and replaced with Dulbecco's Modified Eagle's Medium/F12 containing 0.5% foetal bovine serum and 1% glutamine. Hypoxia was induced by placing cells in a pre-warmed Billups–Rothenburg Modular Incubator Chamber and flushing with 95% N_2, 5% CO_2 for 5 min

(20 l/min). The chamber was placed in a 37°C incubator for 3 h. The chamber was regassed with 95% N_2, 5% CO_2 after the first hour to ensure removal of all the gas that may have been trapped in the plasticware. Following hypoxia, medium was removed and replaced with rat brain microvascular endothelial cell growth media containing either H_2O (no treatment), 100 μM carbenoxolone (non-specific gap junction channel blocker), 200 μM lanthanum chloride ($LaCl_3$, non-specific hemichannel blocker), 50 μM connexin43 mimetic peptide or 50 μM scrambled peptide. Cells were incubated at 37°C, 5% CO_2 for 6 h. Cells were then trypsinized, resuspended in medium and the cell suspension mixed with 0.4% Trypan Blue in order to count the number of viable cells. Cells that had not been exposed to low serum and hypoxia were counted as controls. Viable cell counts were expressed as a percentage of control. Six experiments were performed with three wells per treatment in each experiment. Data from three wells were averaged to obtain the average cell count in each treatment, which was then analysed. Human microvascular endothelial cells (plated at 1.3×10^5 cells/well) in complete media (Dulbecco's Modified Eagle Medium: Nutrient Mixture F-12 containing 10% foetal bovine serum and 1% glutamine) were analysed in the same way. Three experiments were performed with three wells per treatment in each experiment. Data from three wells were averaged to obtain the average cell count in each treatment, which was then analysed.

To confirm endothelial cell death was due to hemichannel opening, a propidium iodide dye uptake assay was carried out (Braet *et al.*, 2003). Rat brain microvascular endothelial cells were plated into a 96-well plate (2×10^4 cells/well) and subjected to hypoxia-reperfusion as described above. Following 1 h of reperfusion, propidium iodide was added to a final concentration of 20 μg/ml. After 30 min, the cells were washed well to remove all propidium iodide from the media and fixed with 10% paraformaldehyde for 5 min. Cells were then imaged on a Leica DM IRB microscope and Leica DFC 425C camera. Six wells were analysed for each experimental group. Four images were taken from every well at ×10 magnification and the number of propidium iodide-positive cells counted. As fixation of the cells alone led to a low level of propidium iodide uptake, normal cells were treated with propidium iodide for the same period and fixed. These were imaged and used to set a threshold so that only cells with a propidium iodide uptake above this level were counted as propidium iodide-positive. A bright field image was taken of each field to determine the total number of cells. The level of propidium iodide uptake was calculated as the number of cells containing propidium iodide as a percentage of the total (% cells with propidium iodide).

Immunohistochemistry

Immunohistochemical techniques were utilized to investigate the effects of ischaemia-reperfusion on connexin43 and GFAP expression and for retinal ganglion cell analysis. Retinas that had one or more quadrants damaged during processing were discarded. For analysis of connexin43 and GFAP, animals were used for each of the following time points after ischaemia-reperfusion and no treatment: 1–2, 4, 8 and 24 h. Retinal whole mounts were used to map retinal ganglion cell counts at 7 and 21 days after ischaemia-reperfusion and no treatment, connexin43 mimetic peptide, or scrambled peptide. Vascular integrity was examined at 4 h after ischaemia-reperfusion and no treatment. Co-localization of connexin43 and vascular endothelial cells was examined in uninjured and ischaemic retinas 8 h after ischaemia-reperfusion.

After euthanasia, eyes were enucleated and the cornea, lens and vitreous humour removed. The dorsal aspect of the retina was notched to retain orientation. The retina and sclera were fixed in 4% paraformaldehyde in phosphate-buffered saline for 60 min at room temperature. The retina was then carefully removed from the sclera and permeabilized via incubation in 0.5% Triton® X-100 in phosphate-buffered saline solution for 15 min at −80°C. Following thorough washing with phosphate-buffered saline, free floating retinas were incubated overnight at 4°C in a primary antibody solution, using rabbit anti-connexin43 (C6219, Sigma Aldrich, 1:2000) and mouse anti-GFAP conjugated to Cy3 (GFAP—C9205, Sigma Aldrich, 1:1000) primary antibodies in 10% normal goat serum and 2% Triton® X-100 in phosphate-buffered saline solution to label connexin43, astrocytes and Muller cells. Primary antibody solution containing rabbit anti-connexin43 and isolectin-B4 conjugated to Alexa594 (I-21413, Molecular Probes, 1:100) was used to double label connexin43 and vascular endothelial cells. Labelling of retinal ganglion cells was achieved with goat anti-Brn3a primary antibody (SC-31984, Santa-Cruz Biotechnology, 1:100) in 2% horse serum and 2% Triton® X-100 in phosphate-buffered saline solution. Vascular integrity was examined by labelling vascular endothelial cells using isolectin-B4 conjugated to Alexa594. After further washing of the retinas with phosphate-buffered saline, a secondary antibody solution was applied for 2 h at room temperature. A goat anti-rabbit Alexa488 secondary antibody (A11034, Invitrogen, 1:1000) labelled the connexin43 primary antibody while a donkey anti-goat Cy3 secondary antibody (705-165-147, Jackson Immuno Research, 1:500) labelled the Brn3a primary antibody. Retinas were incubated in the nuclear marker DAPI (4′,6-diamidino-2-phenylindole) (D9542, Sigma Aldrich) before being mounted onto SuperFrost® Plus slides using Citifluor™ mounting medium, and imaged.

Imaging and quantification

Specimens were examined with an Olympus FV1000 confocal laser scanning microscope. For dye leak experiments, the entire retina was imaged using a ×10 air objective. Absorbance and emission spectra for Evans blue dye have been previously characterized (Saria and Lundberg, 1983). Here, 559 nm excitation was used and emission was viewed with a 575- to 675-nm band filter. Dye leak was consistently spherical or ovoid in shape and the area of dye leak was thus measured using the formula:

$$\text{Area of dye} = r_1 \times r_2 \times \pi,$$

where r_1 and r_2 are dye leak radii in the x and y axes.

Total accumulated dye leak from vessels was measured as the sum of individual dye leak areas.

For connexin43, astrocytosis and retinal ganglion cell density immunohistochemical analysis, two fields in each quadrant of each retina were imaged giving a total of eight images per retina. This method insured similar locations were assessed between different eyes and avoided any possible area bias present in the retina. Connexin43 and GFAP label was imaged using a ×60 oil immersion objective lens and retinal ganglion cell labelling was imaged at ×10 magnification. Voltage and offset settings were adjusted to best discriminate individual antibody labelling and to avoid oversaturation of the image. Quantification was performed using automated spot counts in NIH ImageJ software. For connexin43 quantification, each image was converted to a binary image using a threshold of 30. To separate clusters the watershed algorithm was applied. A particle count was then performed to determine the connexin43 spot count per image. For retinal ganglion cell quantification each image was first filtered with a sharpen filter to delineate cell edges before being converted to a binary image using a threshold of 33. Spots of 1 or 2 pixel^2 that

resulted from noise and artefacts that were clearly not retinal ganglion cell of origin were excluded during particle counts. Retinal ganglion cell density was calculated as the number of retinal ganglion cells per mm^2.

Western blotting

Western blotting was used to determine changes in GFAP expression 8 h after ischaemia-reperfusion injury. Treatment groups included no treatment, systemic connexin43 mimetic peptide perfusion, or scrambled peptide perfusion. Retinas from uninjured animals were used as controls. Two animals were included in each treatment group. The 8-h time point was chosen to coincide with maximum connexin43 upregulation. After euthanasia, eyes were enucleated and the cornea, lens and vitreous humour removed. Retinas were immediately frozen in liquid nitrogen and stored at −20°C until homogenization. Each retina was cut into pieces using iris scissors and placed into 200 µl ice-cold homogenization buffer (150 mM sucrose, 50 mM HEPES pH 7.9, 60 mM KCl, 5 mM EDTA pH 8.0, 1 mM EGTA pH 8.0) containing one complete mini protease inhibitor cocktail tablet (04 693 124 001, Roche) per 10 ml. Tissue was then homogenized using a hand-held homogenizer (5 × 75 mm probe, Pro Scientific Pro 200) for 90 s while being kept on ice. Samples were incubated on ice for 1 h with 1% Triton® X-100, centrifuged at 10 000 rpm for 10 min and the supernatant collected for protein concentration assay.

Sample protein concentrations were determined using the Biorad RC DC™ Protein Assay Kit II (500-0122) following kit instructions. Samples were diluted with homogenization buffer to a standard concentration of 1 µg/µl for western blotting. A 10-µl sample in 10 µl of sample loading dye, and 10 µl of BenchMark™ pre-stained protein ladder (10748-010, Invitrogen) were run on a 10% separating bis-acrylamide gel with 4% stacking gel for 50 min at 170 mV in sodium dodecyl sulphate polyacrylamide gel electrophoresis denaturing buffer (0.2 M glycerine, 25 mM Tris pH 6.8, 35 mM sodium dodecyl sulphate). All eight samples were run on the same gel. Separated proteins and the ladder on the gel were transferred to Hybond™ ECL™ nitrocellulose membrane (RPN2020D, GE Healthcare), and assembled with the gel in a wet transfer apparatus. Transfer was performed at 170 mA for 1 h in cold transfer buffer (25 mM Tris, 192 mM glycine and 20% v/v methanol). The membrane was blocked with 5% non-fat milk powder in TBS-T (containing 20 mM Tris, 137 mM NaCl, 0.1% Tween-20) for 1 h and thoroughly washed (six times for 5 min each in TBS-T). All membranes were labelled with a cocktail of rabbit anti-GFAP antibody (Z0334, Dako, 1:1000) and anti-GAPDH antibody (G9545, Sigma Aldrich, 1:4000) in antibody solution (TBS-T with 2 mM EDTA pH 8.0 and 1% bovine serum albumin) overnight, thoroughly washed, followed by anti-rabbit Ig horse radish peroxidase linked whole antibody (NA934V, Amersham Biosciences, 1:40 000) in antibody solution, then thoroughly washed again. The signal was detected using an Amersham ECL Plus™ Western Blotting Detection System (RPN2132, GE Healthcare) and a Fujifilm LAS 3000 Imager with the chemiluminescence function. A visible light photo of the protein ladder was also taken without moving the membrane.

Equal loading was controlled for by the amount of a house keeping protein GAPDH. The images taken were then analysed with ImageJ. The integrated intensity of connexin43 bands and GAPDH bands was measured, and a relative integrated intensity calculated by dividing the integrated intensity of connexin43 by GAPDH. The average relative integrated intensity of two samples ± SEM in each treatment group from one western blot run was plotted and presented along with four sample lanes. Western blotting of the same samples was repeated four times to confirm consistency of results.

Statistical analysis

Data are given as arithmetic means ± standard error. Statistical comparisons between groups were performed using the Mann–Whitney *U* test (also known as the Wilcoxon test) since data were not normally distributed and normality cannot be restored by transformation. The difference was considered significant when $P < 0.05$. All statistical analysis was performed in IBM SPSS Statistics 19.

Results

Treatment with connexin43 gap junction channel blocker limits vascular leakage

Following retinal ischaemia-reperfusion, extravascular dye leakage was observed within an hour of reperfusion, peaked at 4-h post-ischaemia but continued at 24 h, the longest reperfusion period analysed (Fig. 1). The dye appeared in ovoid patches where it had leaked from compromised vascular endothelium. Retinas from animals that had no Evans blue dye injected were examined to ensure that there was no background fluorescence. Uninjured animals that were injected with Evans blue dye did not exhibit dye leak from the retinal vasculature beyond a few patches resulting from handling, but the vessels were clearly demarcated by the dye within them. Isolectin-B4 labelling of retinal vascular endothelial cells showed tubular and continuous vessels forming an anastomosing vascular network (Fig. 1E). By 4 h following ischaemia-reperfusion, isolectin-B4 labelling revealed clumped vascular membrane material, single endothelial cell layers (as opposed to double track or tube-like structures) and label breaks, indicating endothelial cell loss and vessel rupture (Fig. 1F).

Quantification of dye leak showed that the total accumulated area of leaked dye per retina following ischaemia-reperfusion was significantly greater than in uninjured tissue (10 567 ± 2615 μm^2) at 1–2 h (87 975 ± 30 675 μm^2), 4 h (601 671 ± 234 163 μm^2) and 24 h reperfusion periods (410 143 ± 81 323 μm^2) that received no treatment (Fig. 2). Systemically delivered connexin43 mimetic peptide significantly reduced the total accumulated area of leaked dye at 4 h (86 280 ± 20 099 μm^2) and 24 h (26 671 ± 5655 μm^2) post-ischaemia compared with no treatment at the respective time points. While the total accumulated area of dye leak at 4 h after connexin43 mimetic peptide treatment was still elevated compared to uninjured control animals, it reached only 14% of that in the untreated, ischaemic eyes.

Endothelial cell death and dye uptake secondary to hypoxia is minimized with connexin43 mimetic peptide *in vitro*

In order to investigate mechanisms contributing to vascular leak, rat brain microvascular endothelial cells *in vitro* were exposed to 3 h hypoxia followed by 6 h reperfusion in culture medium containing connexin43 mimetic peptide, scrambled peptide, carbenoxolone, $LaCl_3$, or no treatment. Following hypoxia and

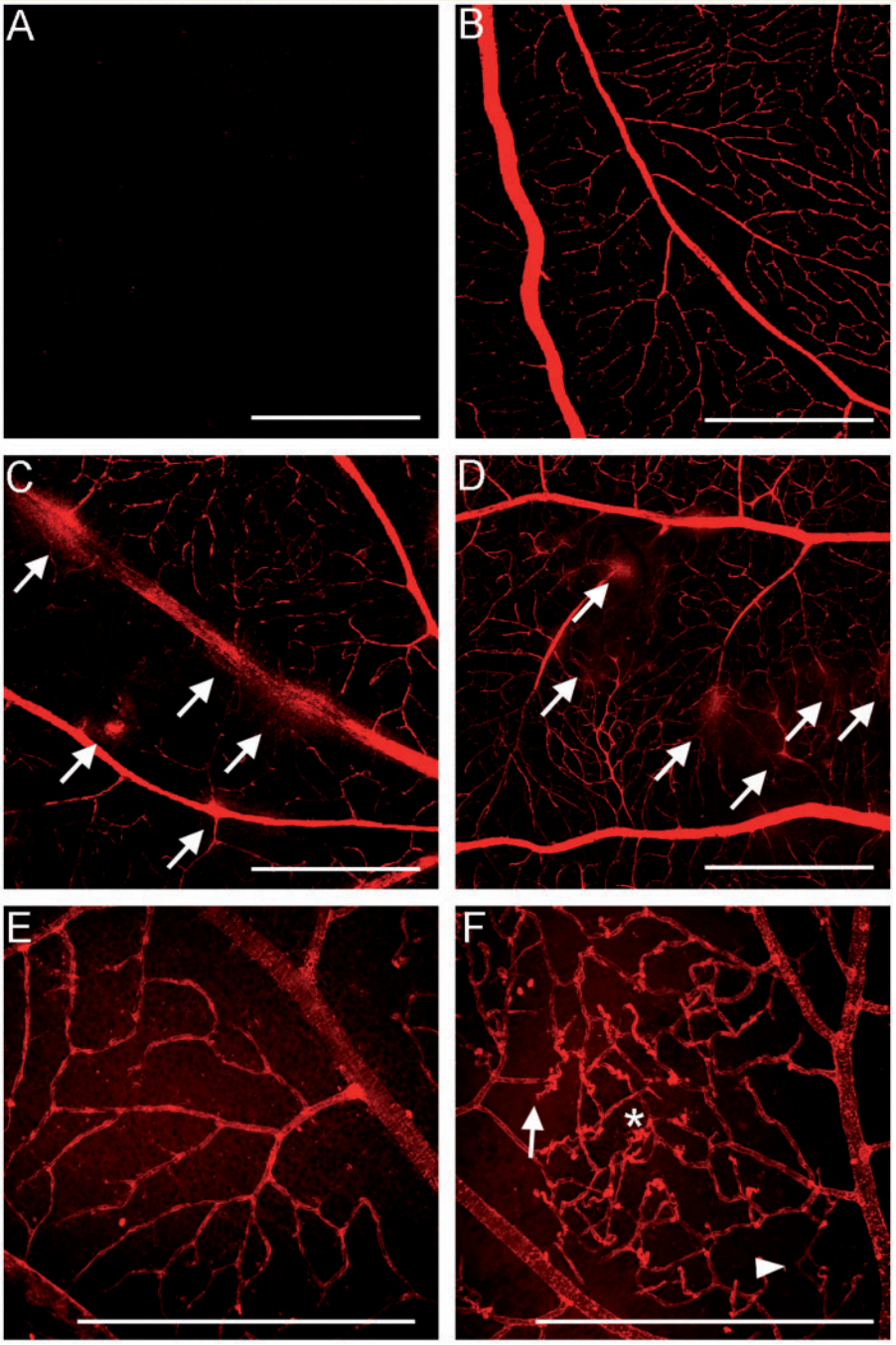

Figure 1 Confocal microscope optical slices of flat mounted retinas displaying Evans blue dye fluorescence (**A**–**D**) and isolectin-B4 labelled blood vessel endothelial cells (**E** and **F**). No endogenous fluorescence was seen in the retina from an animal with no Evans blue dye administered (**A**). Normal blood vessels from an uninjured animal infused with Evans blue dye are seen in (**B**), where the vessels are demarcated by the dye but there is no leakage to the extracellular space. Dye leak from blood vessels (arrows), indicating vascular disruption, was evident at both 4 (**C**) and 24 h (**D**) following retinal ischaemia-reperfusion. Blood vessel endothelial cell labelling with isolectin-B4 from an uninjured animal is seen in **E**. The vessels appear tubular and continuous. At 4 h following ischaemia-reperfusion (**F**) vessels appear fragmented with breaks (arrow), many single membrane structures (arrowhead) and endothelial membrane aggregations (asterisk). Scale bar = 500 μm.

no treatment or scrambled peptide, ~25% of the endothelial cells died compared to control (100 ± 2.9%; no treatment 77.0 ± 4.2% survival; scrambled peptide 76.7 ± 4.3% survival; $P < 0.05$) (Fig. 3A) as assessed by viable cell counts. Addition of either the non-specific gap junction channel blocker carbenoxolone (95.0 ± 1.4%), the hemichannel blocker $LaCl_3$ (95.8 ± 2.0%) or 50 μM connexin43 mimetic peptide (95.6 ± 2.6%) prevented cell death ($P < 0.05$) when compared

to no treatment. In addition, human microvascular endothelial cells were also analysed in a similar manner. Following hypoxia and no treatment or scrambled peptide, ~30% of the endothelial cells died compared to control (100 ± 1.5%; no treatment 70.9 ± 4.3% survival; scrambled peptide 71.8 ± 6.0% survival; $P < 0.05$) as assessed by viable cell counts. Addition of either carbenoxolone (97.0 ± 3.6%), $LaCl_3$ (93.1 ± 4.1%) or 50 μM connexin43 mimetic peptide (93.9 ± 4.8%) prevented cell death ($P < 0.05$) when compared with no treatment.

Hypoxia resulted in connexin43 hemichannel-mediated propidium iodide dye uptake in 19.9 ± 5.0% cells with no treatment or 15.1 ± 2.5% with scrambled peptide (Fig. 3B). Treatment with either carbenoxolone (1.1 ± 0.6%), $LaCl_3$ (1.6 ± 0.6%) or 50 μM connexin43 mimetic peptide (2.0 ± 0.6%) prevented dye uptake ($P < 0.05$) when compared to no treatment.

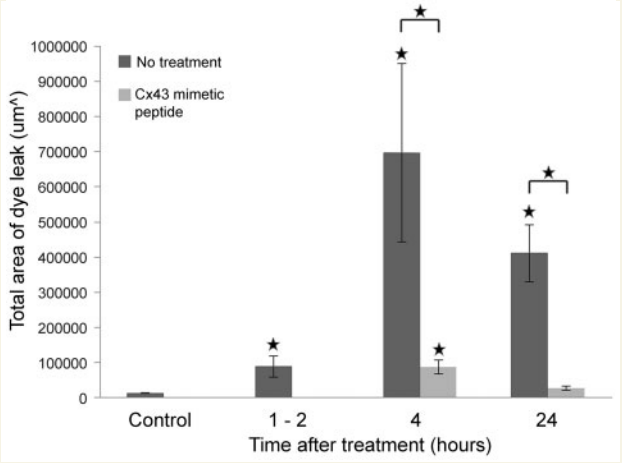

Figure 2 Connexin43 (Cx43) mimetic peptide treatment significantly reduced the total accumulated area of dye leak from blood vessels compared with no treatment at both 4 and 24 h following retinal ischaemia-reperfusion injury. The accumulated dye leak in retinas with no treatment was significantly increased at 1–2, 4 and 24 h following ischaemia-reperfusion compared to uninjured control retinas. Although at 4 h after connexin43 mimetic peptide treatment dye leak remained significantly higher than in uninjured control retinas, it only reached 14% of that in the no treatment ischaemic retinas. Stars denote statistical significance when compared to the control group or compared between groups in brackets; $P < 0.05$.

Connexin43 and glial fibrillary acidic protein response

Quantitative and qualitative changes were observed in connexin43 and GFAP protein expression following retinal ischaemia-reperfusion. Four hours after ischaemia-reperfusion, connexin43 was significantly upregulated in the retina, and co-localized with GFAP positive astrocytes (GFAP also labels Muller cells) and isolectin-B4-positive vascular endothelial cells (Fig. 4). Mean connexin43 spot counts were significantly increased ($P < 0.05$) in the retina at 1–2 h (1854 ± 140), 4 h (3484 ± 224), 8 h (3536 ± 309) and 24 h (3353 ± 320) after ischaemia-reperfusion compared to uninjured retinas (1443 ± 122) (Fig. 5). Since astrocytes wrap around vessels with foot processes onto endothelial cells, blood vessels were clearly outlined with GFAP labelling (Fig. 6). Ischaemia-reperfusion caused patches of localized GFAP upregulation and astrocyte disorganization adjacent to blood vessels within 1 h. In those areas where the vascular endothelium had been disrupted, astrocytic foot processes had lost their normal organized

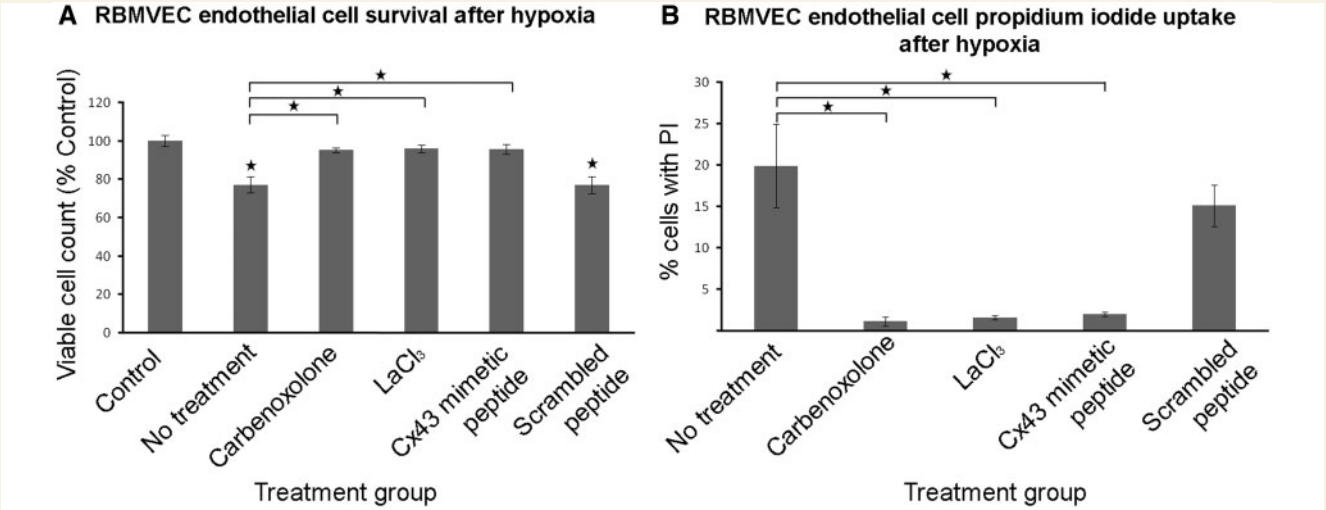

Figure 3 Three hours of hypoxia and 6 h of reperfusion lead to significant endothelial cell death *in vitro* in rat brain microvascular endothelial cells (RBMVEC; **A**). Non-specific gap junction blocker carbenoxolone, non-specific hemichannel blocker $LaCl_3$, and connexin43 (Cx43) mimetic peptide protected endothelial cells against hypoxic injury, with the number of viable cells significantly higher than no treatment, while scrambled peptide did not have any protective effects. The number of viable cells was expressed as percentage of the control without hypoxia. Hypoxia and reperfusion also lead to significant propidium iodide dye uptake into primary rat brain microvascular endothelial cells indicating open hemichannels (**B**). Carbenoxolone, $LaCl_3$ and connexin43 mimetic peptide significantly prevented dye uptake compared to no treatment, indicating hemichannel closure, while scrambled peptide did not have any effect. Stars denote statistical significance when compared to the control group or compared between groups in brackets; $P < 0.05$.

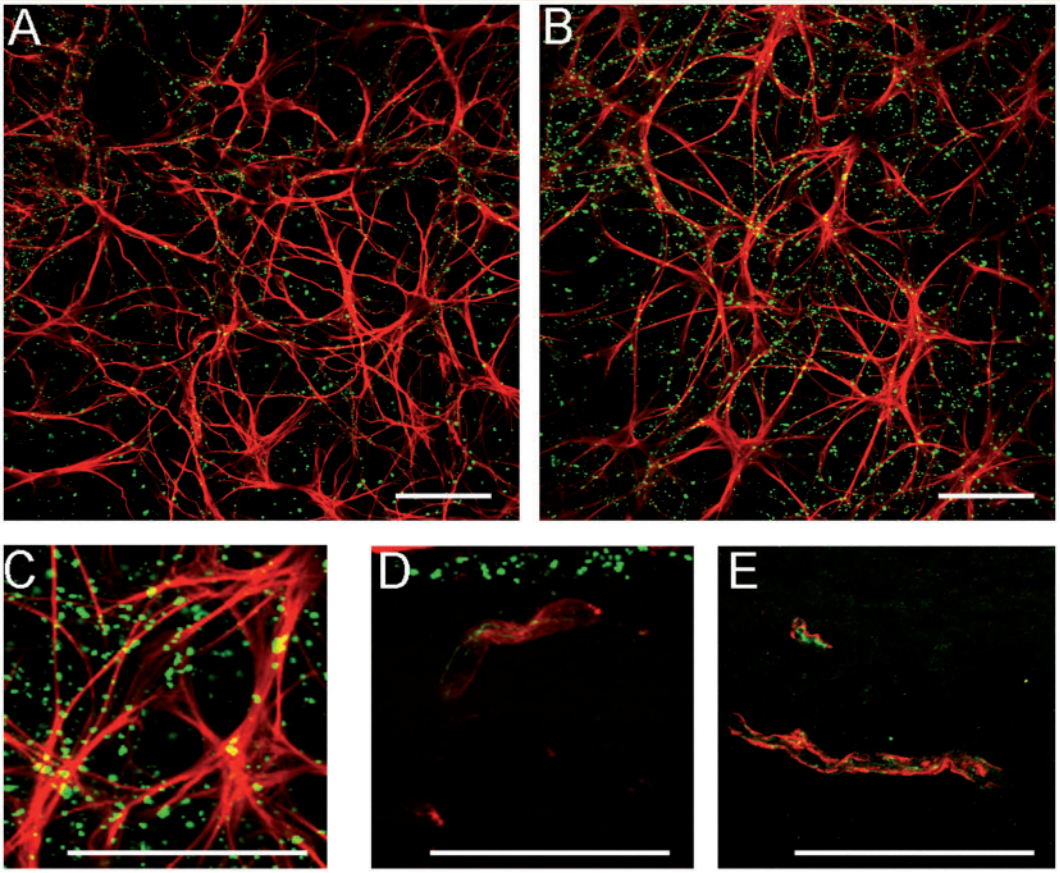

Figure 4 Confocal microscope images of flat mounted retinas labelled for connexin43 (green), GFAP (red, **A–C**) and isolectin-B4 (red, **D** and **E**). An uninjured retina with connexin43 labelling co-localized with astrocyte processes is seen in **A**. Four hours after ischaemia-reperfusion, connexin43 was significantly upregulated in the retina, and co-localized to activated astrocytes that appeared hypertrophied and expressed increased levels of GFAP (**B**). A higher magnification image with connexin43 and GFAP co-localization (yellow spots) is shown in (**C**). Connexin43 labelling (green) was also co-localized with blood vessel endothelial cells (red) in uninjured retina (**D**) and increased in ischaemic retina (**E**) 8 h after ischaemia-reperfusion. Scale bar = 40 μm.

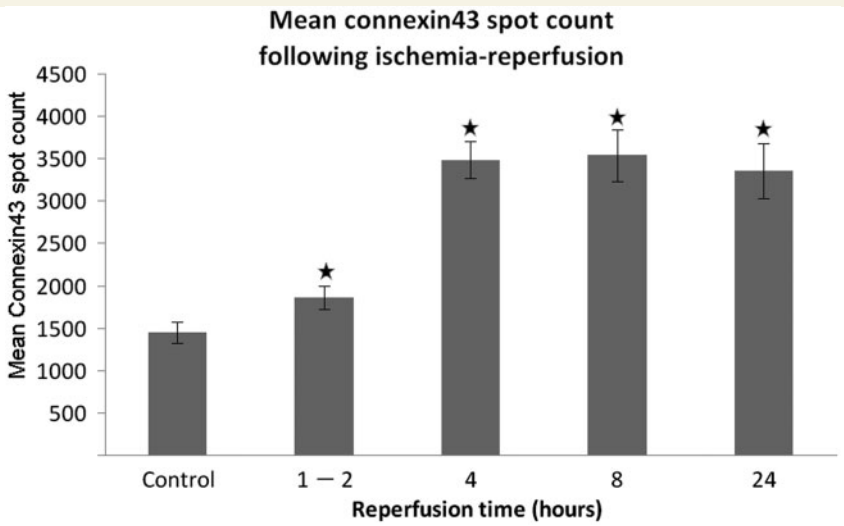

Figure 5 Average connexin43 spot counts in uninjured control retinas and following ischaemia-reperfusion. Connexin43 spot counts were significantly increased in retinas following ischaemia-reperfusion injury at 1–2, 4, 8 and 24 h compared to uninjured control animals. Stars denote statistical significance when compared to the control group; $P < 0.05$.

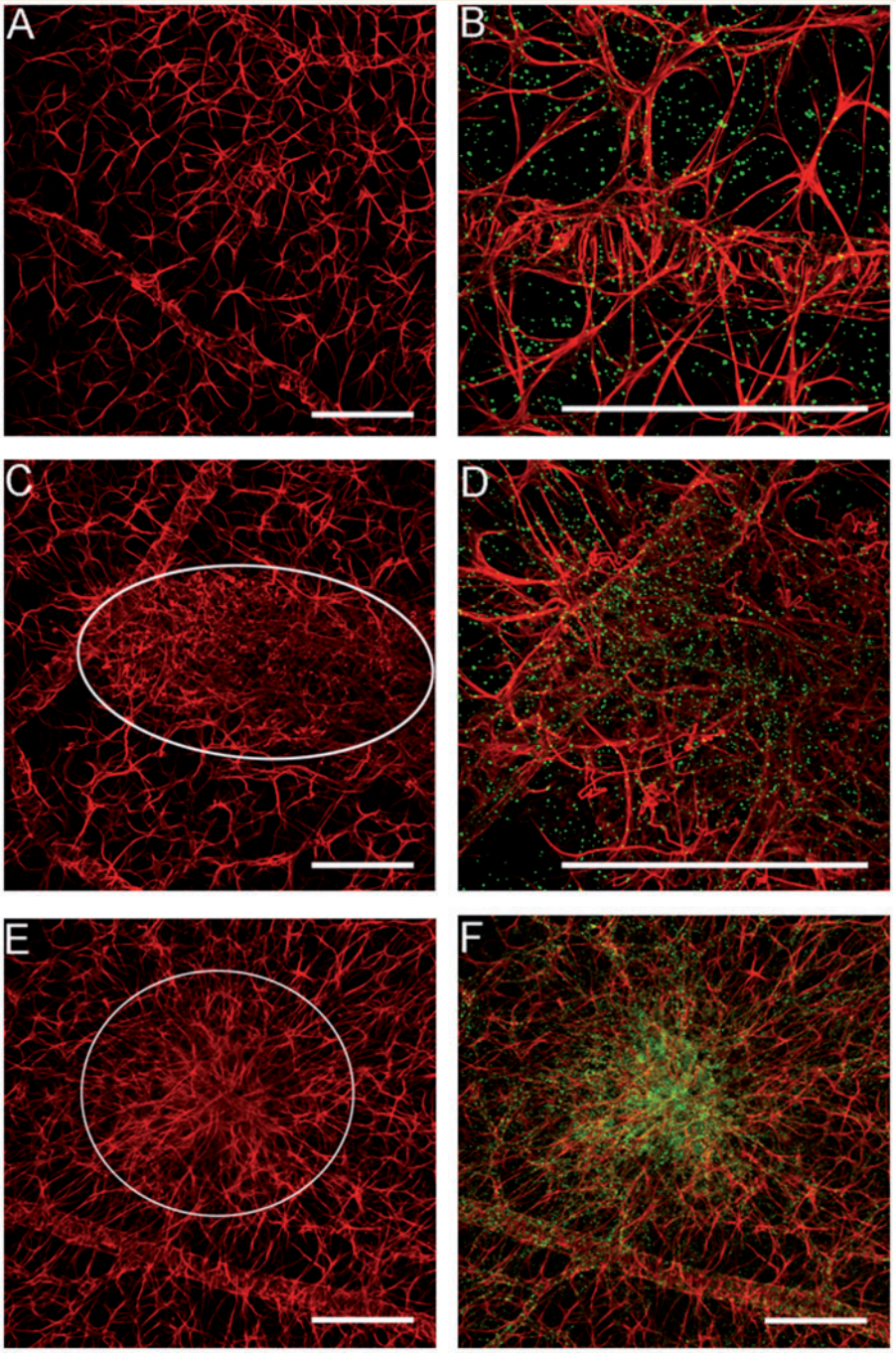

Figure 6 Confocal microscope images of flat mounted retinas labelled for GFAP (red) and connexin43 (green). GFAP expression in a control eye from an uninjured animal showed the astrocyte processes demarcating blood vessels and an orderly arrangement of astrocytes between vessels (**A**). A higher magnification image of the control eye shows the well-organized network of astrocyte processes and their co-localization with connexin43 (**B**). In comparison, ischaemia-reperfusion caused patches of localized GFAP upregulation and astrocyte disorganization (oval area) adjacent to blood vessels within 1–2 h reperfusion (**C**, low magnification with GFAP label and **D**, high magnification with both GFAP and connexin43 labelling). Astrocyte disorganization in localized regions adjacent to blood vessels in the retinal tissue was still evident after 24 h reperfusion (**E**), again accompanied by upregulation of connexin43 expression (**F**). Scale bar = 150 μm.

appearance and the processes appeared within the damaged vessel lumen (seen by sequentially stepping through the confocal *z*-stack shown in Fig. 6D). Astrocyte disorganization in localized regions adjacent to blood vessels in the retinal tissue was still evident 24 h after reperfusion. These localized areas of astrocytosis appeared similar in distribution to the areas of vessel leak observed after Evans blue dye perfusion and correlated with significant upregulation in connexin43 expression. Western blot analysis 8 h

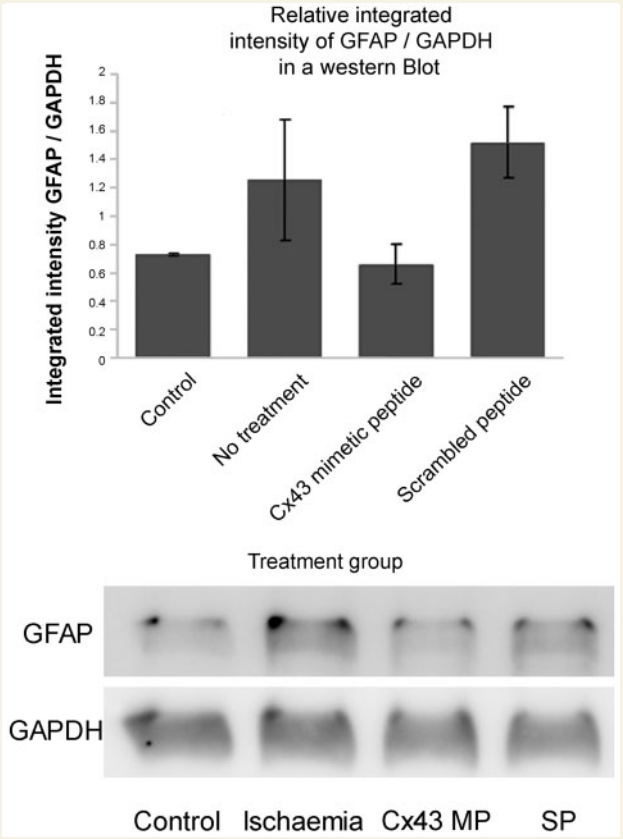

Figure 7 Western blot analysis showing GFAP levels in control retina and 8 h after ischaemia-reperfusion. Ischaemia-reperfusion caused an upregulation of GFAP. Connexin43 (Cx43) mimetic peptide treatment inhibited this upregulation, with GFAP levels remaining at the pre-ischaemia levels. Scrambled peptide was not able to prevent the increase in post-ischaemic GFAP levels. MP = mimetic peptide; SP = scrambled peptide.

after ischaemia-reperfusion confirmed upregulation of GFAP expression (Fig. 7). Connexin43 mimetic peptide treatment inhibited this upregulation whereas scrambled peptide had no effect.

Connexin43 mimetic peptide treatment results in retinal ganglion cell rescue

Following ischaemia-reperfusion, retinal ganglion cell density (number of cells per mm^2) was significantly reduced at both 7 and 21 days in animals that received no treatment (1935 ± 130 and 1971 ± 139, respectively) or treatment with a scrambled peptide (1820 ± 97 and 2094 ± 90, respectively) compared to uninjured controls (3035 ± 258) (Figs 8 and 9). The normal distribution of retinal ganglion cells in flat whole mounts of uninjured retinas is seen in Fig. 8A. Figure 8B shows the retinal ganglion cell distribution in a retina 7 days after ischaemia-reperfusion. Figure 8C and D show the typical appearance of a retina at 7 days of animals treated with connexin43 mimetic peptide and scrambled peptide, respectively. The retinal ganglion cell densities are plotted against time in Fig. 9. Animals treated with a single injection of connexin43 mimetic peptide immediately following ischaemia-reperfusion showed no significant reduction in retinal ganglion cell density at 7 days (2775 ± 158) and 21 days (2611 ± 158) compared to uninjured retinas (Fig. 9).

Discussion

This study provides new information on the pathology of and potential treatment strategies for retinal ischaemia, which may be extrapolated more broadly to CNS ischaemia, chronic inflammatory diseases and trauma. We observed vascular leak peaking at 4-h post ischaemia-reperfusion, which correlated with discrete, localized regions of astrocytosis (and potentially Muller cell activation) and associated connexin43 upregulation. Importantly, this vessel leak was reduced with systemic delivery of connexin43 mimetic peptide. Astrocytosis (as determined by GFAP levels) was similarly attenuated. Furthermore, retinal ganglion cell loss seen at 7- and 21-day post ischaemia-reperfusion was significantly reduced by a single intraperitoneal injection of connexin43 mimetic peptide given immediately after the ischaemic event. We would expect the severity and duration of the insult to affect the number of retinal ganglion cells lost and in our model this was ~35% following 1 h ischaemia. With systemic mimetic delivery, this loss was reduced by two-thirds (down to 9–14%). We suggest that the upregulation of connexin43 immunoreactivity that occurs following ischaemic injury is responsible for the increased vascular leakage and subsequently the inflammatory cascade leading to retinal ganglion cell death. Blocking connexin43 hemichannels has a significant neuroprotective effect.

It is well recognized that the retina, like the brain and spinal cord, responds to ischaemia-reperfusion with both neurodegeneration and increased vascular permeability (Wilson *et al.*, 1995; Zheng *et al.*, 2007; Abcouwer *et al.*, 2010). In a study similar to ours, in which rat retinas were subjected to 45 min of retinal ischaemia followed by reperfusion, Evans blue dye leak from the retinal vasculature was evident at 4 h but continued to 48 h (Abcouwer *et al.*, 2010). An MRI study found that vascular leakage after 60 min of retinal ischaemia lasted for up to 57 days (Wilson *et al.*, 1995). Retinal capillaries were found to start to degenerate, shown with TUNEL (terminal dUTP nick end labelling) cell death labelling, from Day 2, and this became much more pronounced at Day 7 (Zheng *et al.*, 2007). Vascular leakage was also a common feature in studies following hypoxia induced injury to the retina (Kaur *et al.*, 2007, 2008). In the present study, vascular integrity of retinal vessels was shown to be compromised as early as 1 h following ischaemia-reperfusion and continued to the 24-h time point. Administration of connexin43 mimetic peptide markedly reduced the total accumulated amount of leaked at the 4- and 24-h time points.

In the retina and the CNS, connexin43 coupled astrocyte end-foot processes have an intimate relationship with the vasculature surrounding each blood vessel to form a comprehensive gliovascular interface (Kim *et al.*, 2006; Kaur *et al.*, 2008; Kerr *et al.*, 2010). Connexin43 expression on astrocytes surrounding the vasculature may play a role in controlling blood vessel permeability (Simard *et al.*, 2003). One possible mechanism is through

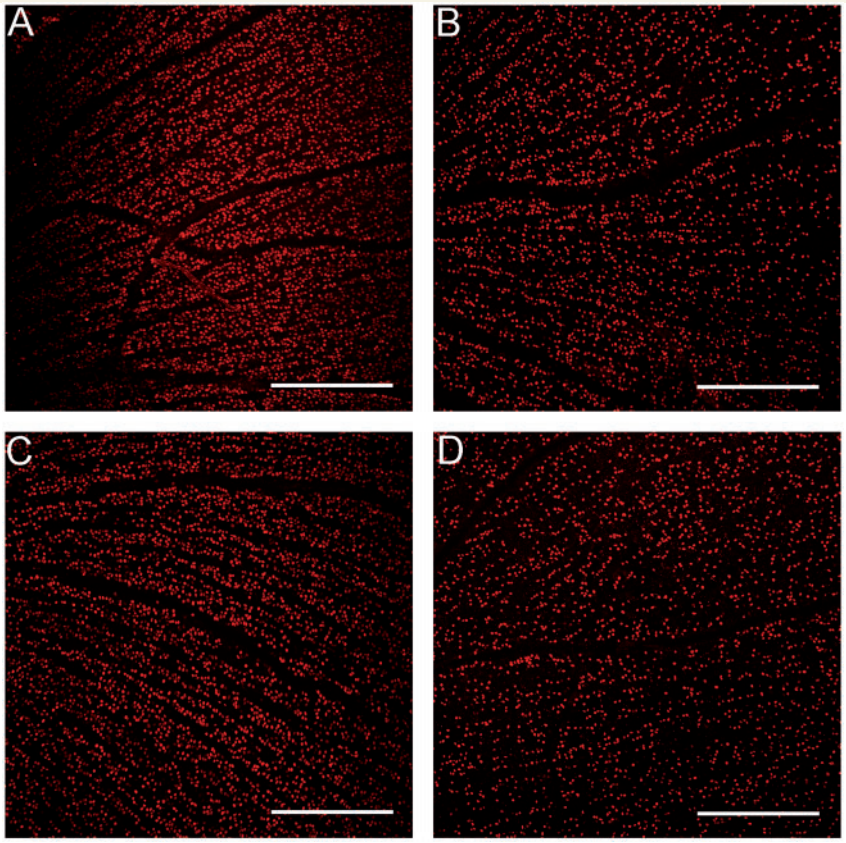

Figure 8 Confocal microscope single optical slice images of flat mounted retinas with Brn3a labelled retinal ganglion cells. In each case, images shown were taken from the mid-periphery of the retina. An uninjured retina is seen with densely packed retinal ganglion cells (**A**). An ischaemic retina 7 days after ischaemia-reperfusion had a reduced retinal ganglion cell density (**B**). Systemic delivery of connexin43 mimetic peptide (**C**) has maintained retinal ganglion cell density at 7 days at almost the same level as uninjured retinas. Scrambled peptide treatment was not neuroprotective and a reduced retinal ganglion cell density was apparent (**D**), with a retinal ganglion cell pattern being similar to that in the ischaemic untreated control (**B**). Scale bar = 1000 μm.

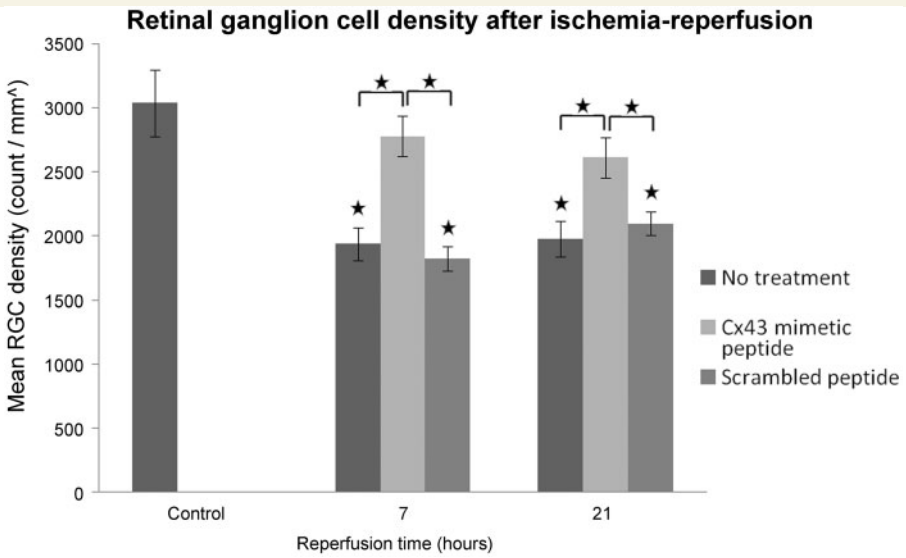

Figure 9 Ischaemia-reperfusion injury lead to a significant loss of retinal ganglion cells (RGC) in the retina at both 7 and 21 days compared to uninjured control. Connexin43 (Cx43) mimetic peptide had a significant rescue effect compared to no treatment at both times whereas scrambled peptide did not. Stars denote statistical significance when compared to the control group or compared between groups in brackets; $P < 0.05$.

astrocytic propagation of calcium waves. Calcium signalling in astrocytes at the blood–retinal barrier is involved in local blood flow regulation and metabolic trafficking (Cornell-Bell *et al.*, 1990; Simard *et al.*, 2003). Calcium waves propagate in the astrocyte-endothelial network via two recognized pathways: inositol trisphosphate spread through connexin43-containing gap junctions between astrocytes and endothelial cells or extracellular ATP spread that may also be facilitated by hemichannel release of ATP (Braet *et al.*, 2001).

Connexin43 expression on endothelial cells (Farahani *et al.*, 2005; Kerr *et al.*, 2010) may, however, independently play an important role in the permeability of blood vessels. Elevation of connexin43 in the walls of small blood vessels has been associated with vascular leakage and extravasation of blood-borne neutrophils within 6 h of a traumatic spinal cord injury (Cronin *et al.*, 2008). Suppression of the connexin43 upregulation using an antisense oligodeoxynucleotide significantly reduced leak of labelled bovine serum albumin and invasion of neutrophils from the blood to the injury site (Cronin *et al.*, 2008). Using an *in vitro* cell ischaemia model, we have demonstrated here that cell death can be mediated directly by opening connexin43 hemichannels in endothelial cells, occurring in the absence of astrocytes. The effect is not species specific. Endothelial cell death was prevented in endothelial cells of both human and rat origin using both non-specific gap junction and hemichannel blockers and specifically the connexin43 mimetic peptide at a concentration that blocks hemichannels but does not uncouple gap junctions (O'Carroll *et al.*, 2008). Ischaemia induced propidium iodide dye uptake was prevented by connexin43 mimetic peptide, indicating the efficacy of the peptide in blocking connexin43 hemichannels. It is probable that *in vivo* endothelial cell death and vessel leak may also occur independently of astrocytosis. Conversely, vascular leak appears to trigger astrocytosis. We identified localized patches of connexin43 upregulation associated with abnormal GFAP expression during the same 1–24 h reperfusion periods following ischaemia, and suggest a causal link between vascular dysfunction and the glial inflammatory response.

A number of factors are said to contribute to blood–brain barrier permeability after hypoxia, in particular tight junction disruption (reviewed in Ballabh *et al.*, 2004; Kaur and Ling, 2008; Yang and Rosenberg, 2011). However, connexin43 hemichannel effects on cytosolic Ca^{2+} concentration and cell volume regulation after ischaemia in a number of cell types signal their vital role in cell injury (reviewed in Rodriguez-Sinovas *et al.*, 2007). Expression of connexin43 in cells results in cell swelling and lysis when the extracellular Ca^{2+} concentration is lowered, a condition promoting hemichannel opening (Rodriguez-Sinovas *et al.*, 2007) and conversely, downregulating connexin43 expression after injury reduces the number of connexin43 hemichannels in the membrane leading to a significant reduction in cell swelling (Cronin *et al.*, 2008; O'Carroll *et al.*, 2008; Zhang *et al.*, 2010). In the vascular endothelium, hypoxia leads directly to endothelial cell loss (Petito, 1979; Danesh-Meyer *et al.*, 2008). We have shown here propidium iodide uptake in endothelial cells and subsequent cell death. Recently, De Bock *et al.* (2011) demonstrated that connexin hemichannel opening leads to blood–brain barrier permeability after a bradykinin-induced inflammatory response. Bradykinin-induced endothelial cell calcium oscillations were blocked both *in vitro* by connexin-specific mimetic peptides, and *in vivo* after systemic peptide delivery. Although they postulate that spatially restricted calcium changes adjacent to tight junctions might be occurring, immunohistochemical localization of occludin and ZO-1 proteins did not reveal tight junction reorganization as the cause of vascular permeability. Regardless, once the blood–brain barrier is breached, astrocytes will become activated (Dietrich *et al.*, 1994; Hirano *et al.*, 1994; Kaur and Ling, 2008) and T cell and monocyte migration augments the inflammatory reaction leading to further tissue damage (Pachter *et al.*, 2003).

Death of retinal ganglion cells following ischaemia-reperfusion is thought to be a result of a complex cascade of events involving glutamate excitotoxicity and inflammatory mediator release (Osborne *et al.*, 2004). Retinal ganglion cells express high levels of kainate and *N*-methyl-D-aspartate glutamate receptors (Brandstatter *et al.*, 1994; Fletcher *et al.*, 2000; Lin *et al.*, 2002), making them especially susceptible to glutamate excitotoxicity (Brandstatter *et al.*, 1994). The disrupted uptake of glutamate into astrocytes following retinal ischaemia-reperfusion may thus play a part in mediating retinal ganglion cell death (Osborne *et al.*, 2004). Nitric oxide is another important neuromediator in the CNS, with increased production by three forms of nitric oxide synthase, endothelial nitric oxide synthase, (Ju *et al.*, 2001; Cheon *et al.*, 2003), neuronal nitric oxide synthase (Gwon *et al.*, 2001; Cheon *et al.*, 2002) and inducible nitric oxide synthase (Neufeld *et al.*, 2002) following retinal ischaemia-reperfusion injury. Although some studies reported a retinal ganglion cell rescue effect due to expression of nitric oxide synthase, the majority of studies found that expression of nitric oxide synthase exacerbates retinal ganglion cell loss, and that inhibition of nitric oxide synthase was protective for retinal ganglion cells following retinal ischaemia-reperfusion (Geyer *et al.*, 1995; Lam and Tso, 1996; Adachi *et al.*, 1998; Ju *et al.*, 2000; Neufeld *et al.*, 2002). Inducible nitric oxide synthase in particular is produced by resident glial cells disrupted by ischaemia-reperfusion injury and neutrophils, which infiltrate the retina following injury and vascular leakage (Hangai *et al.*, 1996; Neufeld *et al.*, 2002). The mechanism of rescue of retinal ganglion cell cells with connexin43 mimetic peptide may therefore be attributed in some part to inhibition of nitric oxide production by reducing retinal glial cell activation and dysfunction. The primary event, however, appears to be hemichannel mediated breaches in the blood–brain barrier; blocking of endothelial hemichannels prevents vascular leak, and the subsequent inflammatory cascade that leads to retinal ganglion cell loss. We have illustrated this pathway schematically in Fig. 10.

In summary, the present findings support the idea that connexin43 upregulation mediates vascular leakage, which is associated with astrocytosis and subsequent retinal ganglion cell loss following retinal ischaemia. Death of retinal ganglion cells after ischaemia-reperfusion follows a complex cascade of events involving glutamate excitotoxicity and inflammatory mediator release including nitric oxide. Our results, however, indicate that an initiating event is vascular endothelial hemichannel related since blocking these channels curtails subsequent events. Modulation of connexin43 after CNS ischaemic-reperfusion injury alleviates vascular leakage and provides significant neuron sparing.

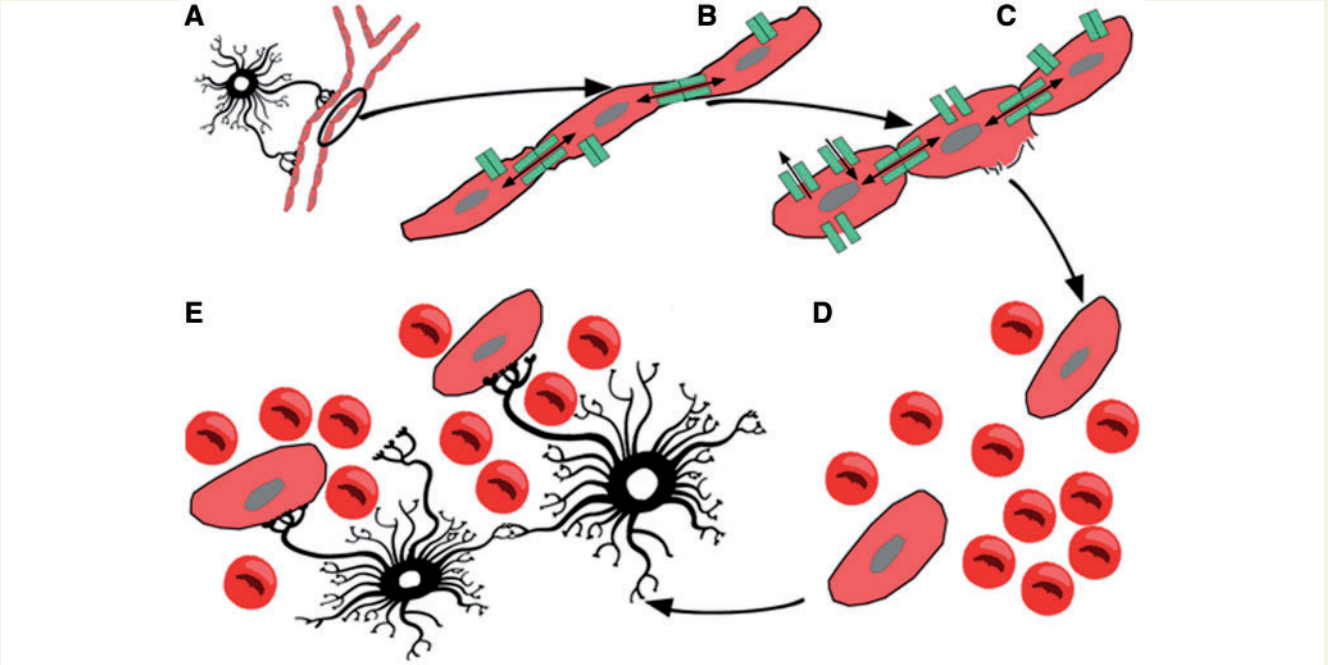

Figure 10 A schematic drawing depicting the initial events following retinal ischaemia that lead ultimately to retinal ganglion cell loss. (**A**) Astrocyte processes interface with the vascular endothelium in order to maintain the neuronal environment and regulate blood flow (reviewed by Kimelberg and Nedergaard, 2010). (**B**) An enlarged view of endothelial cells that are gap junction coupled, with undocked, but closed, hemichannels in the plasma membrane. After ischaemia-reperfusion endothelial connexin expression is upregulated (Kerr *et al.*, 2010 and Fig. 4F) and after insult hemichannels open (Orellana *et al.*, 2009; De Bock *et al.*, 2011). This leads directly to endothelial cell oedema (**C**) and rupture (**D**) (Petito, 1979; Rodriguez-Sinovas *et al.*, 2007; Danesh-Meyer *et al.*, 2008; Fig. 1E and F). Astrocytes then become activated (**E**) (Dietrich *et al.*, 1994*a*; Hirano *et al.*, 1994; Kaur *et al.*, 2006; Fig. 6) and T cell and monocyte migration augments the inflammatory reaction and leads to further tissue damage (Pachter *et al.*, 2003). The subsequent death of retinal ganglion cells following ischaemia-reperfusion is a complex cascade of events involving glutamate excitotoxicity and inflammatory mediator release including nitric oxide (Osborne *et al.*, 2004). Astrocyte gap junction channels also play a role with ATP and glutamate release; inhibition of astrocytic gap junction permeability by octanol for example restricts the flow of neurotoxins that otherwise exacerbate neuronal damage (Rami *et al.*, 2001). The initiating event appears to be vascular endothelial hemichannel-related since block of these hemichannels with connexin43 mimetic peptides reduces astrocytosis, and subsequent downstream retinal ganglion cell loss.

Acknowledgements

We thank Dr Monica Acosta (Department of Optometry, University of Auckland) for advice on the retinal ischaemia reperfusion model used for this study.

Funding

Neurological Foundation of New Zealand and the Stevenson Trust of New Zealand.

References

Abcouwer SF, Lin C-m, Wolpert EB, Shanmugam S, Schaefer EW, Freeman WM, et al. Effects of ischemic preconditioning and bevacizumab on apoptosis and vascular permeability following retinal ischemia–reperfusion injury. Invest Ophthalmol Vis Sci 2010; 51: 5920–33.

Adachi K, Fujita Y, Morizane C, Akaike A, Ueda M, Satoh M, et al. Inhibition of NMDA receptors and nitric oxide synthase reduces ischemic injury of the retina. Eur J Pharmacol 1998; 350: 53–7.

Ballabh P, Braun A, Nedergaard M. The blood-brain barrier: an overview: structure, regulation, and clinical implications. Neurobiol Dis 2004; 16: 1–13.

Braet K, Paemeleire K, D'Herde K, Sanderson MJ, Leybaert L. Astrocyte-endothelial cell calcium signals conveyed by two signalling pathways. Eur J Neurosci 2001; 13: 79–91.

Braet K, Aspeslagh S, Vandamme W, Willecke K, Martin PE, Evans WH, et al. Pharmacological sensitivity of ATP release triggered by photoliberation of inositol-1,4,5-trisphosphate and zero extracellular calcium in brain endothelial cells. J Cell Physiol 2003; 197: 205–13.

Brandstatter JH, Hartveit E, Sassoe-Pognetto M, Wassle H. Expression of NMDA and high-affinity kainate receptor subunit mRNAs in the adult rat retina. Eur J Neurosci 1994; 6: 1100–12.

Cheon EW, Park CH, Kang SS, Cho GJ, Yoo JM, Song JK, et al. Nitric oxide synthase expression in the transient ischemic rat retina: neuroprotection of betaxolol. Neurosci Lett 2002; 330: 265–9.

Cheon EW, Park CH, Kang SS, Cho GJ, Yoo JM, Song JK, et al. Change in endothelial nitric oxide synthase in the rat retina following transient ischemia. Neuroreport 2003; 14: 329–33.

Cornell-Bell AH, Finkbeiner SM, Cooper MS, Smith SJ. Glutamate induces calcium waves in cultured astrocytes: long-range glial signaling. Science 1990; 247: 470–3.

Cronin M, Anderson PN, Cook JE, Green CR, Becker DL. Blocking connexin43 expression reduces inflammation and improves functional recovery after spinal cord injury. Mol Cell Neurosci 2008; 39: 152–60.

Danesh-Meyer HV, Huang R, Nicholson LFB, Green CR. Connexin43 antisense oligodeoxynucleotide treatment down-regulates the inflammatory response in an in vitro interphase organotypic culture model of optic nerve ischaemia. J Clin Neurosci 2008; 15: 1253–63.

Das S, Lin D, Jena S, Shi A, Battina S, Hua DH, et al. Protection of retinal cells from ischemia by a novel gap junction inhibitor. Biochem Biophys Res Commun 2008; 373: 504–8.

De Bock M, Culot M, Wang N, Bol M, Decrock E, De Vuyst E, et al. Connexin channels provide a target to manipulate brain endothelial calcium dynamics and blood-brain barrier permeability. J Cereb Blood Flow Metab 2011; 31: 1942–57.

DePaola N, Davies PF, Pritchard WF Jr, Florez L, Harbeck N, Polacek DC. Spatial and temporal regulation of gap junction connexin43 in vascular endothelial cells exposed to controlled disturbed flows in vitro. Proc Natl Acad Sci USA 1999; 96: 3154–9.

Farahani R, Pina-Benabou MH, Kyrozis A, Siddiq A, Barradas PC, Chiu F-C, et al. Alterations in metabolism and gap junction expression may determine the role of astrocytes as "good samaritans" or executioners. Glia 2005; 50: 351–61.

Fletcher EL, Hack I, Brandstatter JH, Wassle H. Synaptic localization of NMDA receptor subunits in the rat retina. J Comp Neurol 2000; 420: 98–112.

Frantseva MV, Kokarovtseva L, Perez Velazquez JL. Ischemia-induced brain damage depends on specific gap-junctional coupling. J Cereb Blood Flow Metab 2002a; 22: 453–62.

Frantseva MV, Kokarovtseva L, Naus CG, Carlen PL, MacFabe D, Perez Velazquez JL. Specific gap junctions enhance the neuronal vulnerability to brain traumatic injury. J Neurosci 2002b; 22: 644–53.

Garcia-Dorado D, Inserte J, Ruiz-Meana M, Gonzalez MA, Solares J, Julia M, et al. Gap junction uncoupler heptanol prevents cell-to-cell progression of hypercontracture and limits necrosis during myocardial reperfusion. Circulation 1997; 96: 3579–86.

Geyer O, Almog J, Lupu-Meiri M, Lazar M, Oron Y. Nitric oxide synthase inhibitors protect rat retina against ischemic injury. FEBS Lett 1995; 374: 399–402.

Goodenough DA, Paul DL. Beyond the gap: functions of unpaired connexon channels. Nat Rev Mol Cell Biol 2003; 4: 285–94.

Gwon JS, Ju WK, Park SJ, Kim IB, Lee MY, Oh SJ, et al. The regulatory expression of neuronal nitric oxide synthase in the ischemic rat retina. Neuroreport 2001; 12: 3385–9.

Hangai M, Yoshimura N, Hiroi K, Mandai M, Honda Y. Inducible nitric oxide synthase in retinal ischemia-reperfusion injury. Exp Eye Res 1996; 63: 501–9.

Haupt C, Witte OW, Frahm C. Temporal profile of connexin 43 expression after photothrombotic lesion in rat brain. Neuroscience 2007; 144: 562–70.

Hawat G, Benderdour M, Rousseau G, Baroudi G. Connexin 43 mimetic peptide Gap26 confers protection to intact heart against myocardial ischemia injury. Pflugers Arch 2010; 460: 583–92.

Hossain MZ, Peeling J, Sutherland GR, Hertzberg EL, Nagy JI. Ischemia-induced cellular redistribution of the astrocytic gap junctional protein connexin43 in rat brain. Brain Res 1994; 652: 311–22.

Ju WK, Gwon JS, Kim KY, Oh SJ, Kim SY, Chun MH. Up-regulated eNOS protects blood–retinal barrier in the L-arginine treated ischemic rat retina. Neuroreport 2001; 12: 2405–9.

Ju WK, Kim KY, Park SJ, Park DK, Park CB, Oh SJ, et al. Nitric oxide is involved in sustained and delayed cell death of rat retina following transient ischemia. Brain Res 2000; 881: 231–6.

Kaur C, Ling EA. Blood brain barrier in hypoxic-ischemic conditions. Curr Neurovasc Res 2008; 5: 71–81.

Kaur C, Foulds WS, Ling EA. Blood-retinal barrier in hypoxic ischaemic conditions: Basic concepts, clinical features and management. Prog Retinal Eye Res 2008; 27: 622–47.

Kaur C, Sivakumar V, Yong Z, Lu J, Foulds WS, Ling EA. Blood-retinal barrier disruption and ultrastructural changes in the hypoxic retina in adult rats: the beneficial effect of melatonin administration. J Pathol 2007; 212: 429–39.

Kerr NM, Johnson CS, de Souza CF, Chee K-S, Good WR, Green CR, et al. Immunolocalization of gap junction protein connexin43 in the human retina and optic nerve. Invest Ophthalmol Vis Sci 2010; 51: 4028–34.

Kim JH, Kim JH, Park JA, Lee S-W, Kim WJ, Yu YS, et al. Blood-neural barrier: intercellular communication at glio-vascular interface. J Biochem Mol Biol 2006; 39: 339–45.

Kimelberg HK, Nedergaard M. Functions of astrocytes and their potential as therapeutic targets. Neurotherapeutics 2010; 7: 338–53.

Lam TT, Tso MO. Nitric oxide synthase (NOS) inhibitors ameliorate retinal damage induced by ischemia in rats. Res Commun Mol Pathol Pharmacol 1996; 92: 329–40.

Lee IH, Eva L, Ole K, Johan W, Lars O. Glial and neuronal connexin expression patterns in the rat spinal cord during development and following injury. J Comp Neurol 2005; 489: 1–10.

Lin B, Martin PR, Grunert U. Expression and distribution of ionotropic glutamate receptor subunits on parasol ganglion cells in the primate retina. Vis Neurosci 2002; 19: 453–65.

Lin JH, Weigel H, Cotrina ML, Liu S, Bueno E, Hansen AJ, et al. Gap-junction-mediated propagation and amplification of cell injury. Nat Neurosci 1998; 1: 494–500.

Nagy JI, Rash JE. Connexins and gap junctions of astrocytes and oligodendrocytes in the CNS. Brain Res Rev 2000; 32: 29–44.

Nakase T, Yoshida Y, Nagata K. Enhanced Connexin 43 immunoreactivity in penumbral areas in the human brain following ischemia. Glia 2006; 54: 369–75.

Nakase T, Sohl G, Theis M, Willecke K, Naus CCG. Increased apoptosis and inflammation after focal brain ischemia in mice lacking connexin43 in astrocytes. Am J Pathol 2004; 164: 2067–75.

Naus CC, Bechberger JF, Caveney S, Wilson JX. Expression of gap junction genes in astrocytes and C6 glioma cells. Neurosci Lett 1991; 126: 33–6.

Naus CC, Ozog MA, Bechberger JF, Nakase T. A neuroprotective role for gap junctions. Cell Commun Adhes 2001; 8: 325–8.

Neufeld AH, Kawai Si, Das S, Vora S, Gachie E, Connor JR, et al. Loss of retinal ganglion cells following retinal ischemia: the role of inducible nitric oxide synthase. Exp Eye Res 2002; 75: 521–8.

O'Carroll SJ, Alkadhi M, Nicholson LF, Green CR. Connexin 43 mimetic peptides reduce swelling, astrogliosis, and neuronal cell death after spinal cord injury. Cell Commun Adhes 2008; 15: 27–42.

Ohsumi A, Nawashiro H, Otani N, Ooigawa H, Toyooka T, Yano A, et al. Alteration of gap junction proteins (connexins) following lateral fluid percussion injury in rats. Acta Neurochir Suppl 2006; 96: 148–50.

Orellana JA, Saez PJ, Shoji KF, Schalper KA, Palacios-Prado N, Velarde V, et al. Modulation of brain hemichannels and gap junction channels by pro-inflammatory agents and their possible role in neurodegeneration. Antioxid Redox Signal 2009; 11: 369–99.

Osborne NN, Casson RJ, Wood JP, Chidlow G, Graham M, Melena J. Retinal ischemia: mechanisms of damage and potential therapeutic strategies. Prog Retin Eye Res 2004; 23: 91–147.

Pachter JS, de Vries HE, Fabry Z. The blood-brain barrier and its role in immune privilege in the central nervous system. J Neuropathol Exp Neurol 2003; 62: 593–604.

Petito CK. Early and late mechanisms of increased vascular permeability following experimental cerebral infarction. J Neuropathol Exp Neurol 1979; 38: 222–34.

Rami A, Volkmann T, Winckler J. Effective reduction of neuronal death by inhibiting gap junctional intercellular communication in a rodent model of global transient cerebral ischemia. Exp Neurol 2001; 170: 297–304.

Rawanduzy A, Hansen A, Hansen TW, Nedergaard M. Effective reduction of infarct volume by gap junction blockade in a rodent model of stroke. J Neurosurg 2009; 87: 916–20.

Rodriguez-Sinovas A, Cabestrero A, Lopez D, Torre I, Morente M, Abellan A, et al. The modulatory effects of connexin 43 on cell death/survival beyond cell coupling. Prog Biophys Mol Biol 2007; 94: 219–32.

Rouach N, Avignone E, Meme W, Koulakoff A, Venance L, Blomstrand F, et al. Gap junctions and connexin expression in the normal and pathological central nervous system. Biol Cell 2002; 94: 457–75.

Shen W, Li S, Chung SH, Gillies MC. Retinal vascular changes after glial disruption in rats. J Neurosci Res 2010; 88: 1485–99.

Simard M, Arcuino G, Takano T, Liu QS, Nedergaard M. Signaling at the gliovascular interface. J Neurosci 2003; 23: 9254–62.

Sun D, Vingrys AJ, Kalloniatis M. Metabolic and functional profiling of the ischemic/reperfused rat retina. The J Comp Neurol 2007; 505: 114–30.

Wilson CA, Berkowitz BA, Funatsu H, Metrikin DC, Harrison DW, Lam MK, et al. Blood-retinal barrier breakdown following experimental retinal ischemia and reperfusion. Exp Eye Res 1995; 61: 547–57.

Yang Y, Rosenberg GA. Blood-brain barrier breakdown in acute and chronic cerebrovascular disease. Stroke 2011; 42: 3323–8.

Yeh H-I, Lai Y-J, Chang H-M, Ko Y-S, Severs NJ, Tsai C-H. Multiple Connexin Expression in Regenerating Arterial Endothelial Gap Junctions. Arterioscler Thromb Vasc Biol 2000; 20: 1753–62.

Yoon JJ, Green CR, O'Carroll SJ, Nicholson LF. Dose-dependent protective effect of connexin43 mimetic peptide against neurodegeneration in an ex vivo model of epileptiform lesion. Epilepsy Res 2010; 92: 153–62.

Zahs KR, Kofuji P, Meier C, Dermietzel R. Connexin immunoreactivity in glial cells of the rat retina. The J Comp Neurol 2003; 455: 531–46.

Zhang J, O'Carroll SJ, Wu A, Nicholson LF, Green CR. A model for ex vivo spinal cord segment culture–a tool for analysis of injury repair strategies. J Neurosci Methods 2010; 192: 49–57.

Zheng L, Gong B, Hatala DA, Kern TS. Retinal ischemia and reperfusion causes capillary degeneration: similarities to diabetes. Invest Ophthalmol Vis Sci 2007; 48: 361–7.

Zhou Y, Shi G, Zheng J, Huang Z, Gao F, Zhang Y, et al. The protective effects of Egr-1 antisense oligodeoxyribonucleotide on cardiac microvascular endothelial injury induced by hypoxia-reoxygenation. Biochem Cell Biol 2010; 88: 687–95.